

## Research Article

Amruta Yadav, Ajay Gajbhiye, Dhiraj Agrawal\*, Khalid Ansari\*, Abdullah H. Alsabhan, Krishna Prakash Arunachalam, Siva Avudaiappan\*, Nelson Maureira-Carsalade\*, and Osamah J. Alsareji

# Mechanical, durability, and microstructure analysis of concrete made with metakaolin and copper slag for sustainable construction

<https://doi.org/10.1515/rams-2025-0138>  
received October 06, 2024; accepted July 18, 2025

**Abstract:** The upsurge in urbanization steered a substantial proliferation in the demand for concrete in the construction industry. As a result, there is a higher demand for cement and fine aggregate, as constituents of concrete. The detrimental effect of cement generation on the environment has been witnessed over the last 4–5 decades. Similarly, the increased demand for fine aggregate has led to extensive extraction of river sand, which results in negative impacts on the environment. Utilizing industrial waste materials like copper slag (CS) and mineral admixtures such as metakaolin

(MK) in eco-friendly concrete production can help reduce this environmental impact. The primary objective of this research is to examine the impact on the mechanical and durability properties of concrete when using CS as a partial replacement for sand, combined with MK as a partial replacement for cement. To evaluate the mechanical characteristics of concrete, tests were conducted to measure split tensile strength, compressive strength, and flexural strength, and its durability was assessed via a rapid chloride ion penetration test. The microstructural analysis of concrete was also performed using scanning electron microscopy and energy dispersive spectroscopy. The optimum percentages of the MK and CS were as fractional switches of cement and sand, respectively, were assessed using the response surface methodology (RSM). The optimal strengths were found at 15% MK and 31.533% CS, while experimentally, the best performance of modified concrete was obtained at 30% CS. The experimental findings and predicted values from the RSM model showed a strong correlation with  $R$ -squared ( $R^2$ ) values obtained as 0.9880 and 0.9552 for compressive and flexural strengths, respectively. The findings have significant implications, as they provide a sustainable alternative to sand while enhancing the performance and longevity of concrete structures.

\* Corresponding author: **Dhiraj Agrawal**, Department of Civil Engineering, Yeshwantrao Chavan College of Engineering, Nagpur, India, e-mail: dgagrwal@ycce.edu

\* Corresponding author: **Khalid Ansari**, Department of Civil Engineering, Yeshwantrao Chavan College of Engineering, Nagpur, India, e-mail: ksansari@ycce.edu

\* Corresponding author: **Siva Avudaiappan**, Departamento de Ciencias de la Construcción, Facultad de Ciencias de la Construcción Ordenamiento Territorial, Universidad Tecnológica Metropolitana, Santiago, Chile, e-mail: s.avudaiappan@utem.cl

\* Corresponding author: **Nelson Maureira-Carsalade**, Departamento de Ingeniería Civil, Universidad Católica de la Santísima Concepción, Concepción, 4090541, Chile, e-mail: nmaureira@ucsc.cl

**Amruta Yadav:** Department of Civil Engineering, Yeshwantrao Chavan College of Engineering, Nagpur, India, e-mail: amruta1227@gmail.com

**Ajay Gajbhiye:** Department of Civil Engineering, Yeshwantrao Chavan College of Engineering, Nagpur, India, e-mail: argajbhiye@ycce.edu

**Abdullah H. Alsabhan:** Department of Civil Engineering, College of Engineering, King Saud University, P.O. Box 800, Riyadh, 12372, Saudi Arabia, e-mail: aalsabhan@ksu.edu.sa

**Krishna Prakash Arunachalam:** Departamento de Ciencias de la Construcción, Facultad de Ciencias de la Construcción Ordenamiento Territorial, Universidad Tecnológica Metropolitana, Santiago, Chile, e-mail: k.prakash@utem.cl

**Osamah J. Alsareji:** Sustainability Solutions Research Lab, Faculty of Engineering, University of Pannonia, Egyetem Str. 10, Veszprém H, 8200, Hungary, e-mail: osamah.al-sareji@phd.uni-pannon.hu

## 1 Introduction

The construction industry requires three essential ingredients: aggregate, sand, and cement. Cement and sand are two crucial elements in making concrete, which significantly impact mixed design, and strength is primarily determined by cement paste quality [1,2]. The cement manufacturing process includes calcination, a chemical reaction that releases substantial amounts of carbon dioxide

into the air by adding to greenhouse gas emissions and harming the environment [3]. Conventional concrete (CC) typically has low strength, durability, and workability, along with high fragility, which can negatively impact the performance and weight of structural elements [4,5].

These environmental issues highlight the need for sustainable substitutes for these materials in the construction industry. Industrialization is essential for the nation's development. Annually, industrial sectors generate substantial quantities of waste that have resulted in a concomitant increase in both the volume and diversity of waste produced, and in this context, slag-based geopolymers emerge as a promising green alternative to conventional concrete, offering improved performance in aggressive sulfate environments, as demonstrated by a comprehensive comparative study of mechanical and durability properties [6]. In developing economies, the management of power plant byproducts such as fly ash, bottom ash, and biomass ash plays a pivotal role in advancing circular economy principles within sustainable construction practices, and aligning with this approach, another study carried out by Ashish investigates the effective utilization of marble powder combined with supplementary cementitious materials like metakaolin (MK) and silica fume, demonstrating enhanced strength and durability properties of concrete while maintaining favorable setting and soundness characteristics in blended cement pastes [7]. This approach not only mitigates environmental risks but also enhances resource efficiency and economic sustainability [8]. Another study conducted by Gill *et al.* presents a unified empirical equation to non-destructively predict geopolymers concrete strength using UPV, AAL/B ratio, and density with high accuracy [9]. Copper slag (CS) is a mining waste product that is extracted while producing copper. It is created in gigantic amounts when copper is extracted [10]. Approximately 2.23 million tonnes of CS are produced for every million tonnes of extracted copper ore [11–13]. A major environmental concern is the disposal of such a massive amount of waste produced by the industries. In the near future, an additional challenge triggered by the weakening of natural aggregates will need a viable solution; wastes from the mining industry can be employed as a non-natural aggregate [14,15]. CS can be utilized as an aggregate or as a fractional substitute for cement in concrete due to its distinctive mechanical and chemical qualities. CS has several beneficial mechanical properties when used as aggregate, such as good stability, abrasion resistance, and soundness characteristics. Additionally, due to the presence of other oxides such as  $\text{SiO}_2$ ,  $\text{Fe}_2\text{O}_3$ , and  $\text{Al}_2\text{O}_3$ , as well as a low  $\text{CaO}$  level, CS displays pozzolanic abilities [16]. It is granular and shiny, and when added to

concrete, it improves the material's strength, durability, workability, and other properties [10,17]. The addition of CS from 0 to 100% improved the workability of the concrete and nearly raised its density by 5%. However, in high-performance concrete, segregations and bleeding at larger substitution levels of 80 and 100% CS were observed [11,18].

Nevertheless, the cement hydration and manufacturing processes generate a substantial amount of heat and release carbon dioxide, a greenhouse gas that exacerbates global warming and climate change [19]. Also, Karatas *et al.* highlighted the environmental benefits of alkali-activated metakaolin cement as a sustainable alternative to Portland cement, which is responsible for approximately 7% of the global  $\text{CO}_2$  emissions [20]. Kaolinite, a clay mineral, is transformed into MK through dihydroxylation [21]. In addition to being frequently utilized in the manufacturing of ceramics, MK can also be substituted for cement in concrete. Because of its excellent pozzolanic properties, the MK material can serve as a cement substitute to create high-performance concrete [22]. MK is a synthetic pozzolana that is produced by heating kaolinite clays to between 700 and 850°C. The incorporation of MK enhances the mechanical and durability characteristics of concrete because of its high pozzolanic activity [18,23]. Arslan *et al.* found that the SCGC mixtures exhibited significant strength gains, particularly in the first 24 h of curing. Ambient-cured GBFS-based mixtures showed strength increases ranging from 10.39 to 26.49% after 24 h, while 28-day strength gains were lower, between 3.04 and 9.19% [24]. Major constituents of MK include amorphous silica and amorphous alumina, which react with calcium hydroxide (CH) and water to yield primarily calcium aluminate hydrates and aluminum silicate hydrates [23]. At all ages up to 180 days, the concrete containing 10% MK was stronger than the control concrete [22]. Note that impurities in MK can limit its reactivity, leading to lower-than-expected strength outcomes [25,26]. Concrete can be made in large amounts without the use of cement and sand through the utilization of industrial wastes such as GGBS, MK, and CS [27–30]. By incorporating MK, concrete achieves lower permeability and greater strength, minimizes chloride ion penetration and water requirements, and improves workability [31]. The addition of 10% MK reduces the workability of concrete containing CS from the River Beas as fine aggregates, although workability increases with higher CS content [32]. Also, the studies carried out show that the inclusion of waste tire aggregates (WTA) and MK significantly improved the mechanical properties of slag/MK-based rubberized semi-lightweight geopolymers composites. With a mixture of 60% WTA and 10% MK, a compressive strength of 25.10 MPa was achieved at a curing temperature of 100°C [33].

It is evident from the research background that several studies have been carried out on CS as a substitute for natural sand (NS) and MK as a partial cement replacement. Concrete with 30% CS replacement exhibited a more compact microstructure than conventional concrete, confirming that the AAM concrete with a higher Si/Al ratio had a more densely packed structure [34]. The potential for using CS, particularly at a 30% level, in micro surfacing treatments is substantial, as it enhances asphalt performance with respect to the curing time, abrasion resistance, and both vertical and lateral displacements due to its angularity and elevated  $Fe_2O_3$  and  $SiO_2$  percentages [35]. Zhang *et al.* showed that using CS as an supplementary cementitious material (SCM) poses no significant environmental risks, as the leaching concentrations of heavy metals in CS comply with regulatory limits. This finding supports the safe use of CS in the construction materials [25].

However, several research studies provided insights into how these materials behave under elevated temperatures, including calcined kaolin and MK, which improve the compressive strength of self-compacting concrete (SCMs) when exposed to high temperatures [36]. For instance, mortars with MK showed increased compressive strength at moderate temperatures (up to 200°C) due to enhanced pozzolanic activity, which contributes to a denser microstructure [37,38]. However, at very high temperatures (e.g., 1,000°C), MK-based SCMs may experience significant strength loss due to microstructural degradation. This transformation results in an amorphous phase that contributes to improved pozzolanic reactivity and mechanical performance at elevated temperatures [39]. MK-based geopolymers also exhibit superior thermal resistance, maintaining structural integrity and reducing cracking tendencies at temperatures above 200°C [40,41]. The relationship of various investigations related to mechanical, durability, and analysis of concrete made with MK and CS for Sustainable Construction is shown in Figure 1 as a cluster diagram from recent years [1–32] with the help of VOS viewers software (v.19).

To bridge the demand–supply gap of raw materials in the construction industry and address the disposal issues of industrial wastes like CS, incorporating such by-products into concrete offers a sustainable solution, and in this direction, fly ash-based geopolymer concrete with alcocofine emerges as an eco-friendly alternative, demonstrating enhanced workability and compressive strength even at ambient conditions, making it suitable for both general and precast concrete applications [42,43]. Utilizing waste materials reduces the cost of concrete, and recycling waste has been considered to be the most environmentally friendly approach to solve the waste disposal challenge

[44–48]. Because of this, the current study attempts to mitigate environmental impacts by partially replacing cement with MK and sand with CS in sustainable concrete production, and in line with this approach, Ashish and Verma explored the potential of industrial symbiosis by utilizing waste foundry sand as a viable resource in self-compacting concrete, revealing improved strength and microstructural properties over time while maintaining environmental safety through leaching analysis [49].

Previous research has highlighted the potential of using industrial byproducts like CS and MK in concrete to enhance its mechanical properties and sustainability. However, these studies often faced limitations in terms of achieving strength using CS or MK individually, rather than in combination. Also, optimal replacement percentages for both CS and MK in combination were not well established. Therefore, the primary aim of this study is to explore the use of CS as a partial replacement for sand and MK as a partial replacement for cement in concrete [50]. This study aims to overcome these limitations by conducting a comprehensive analysis of the mechanical and durability properties of concrete and optimizing response surface methodology (RSM) to determine the optimal proportions of CS and MK for enhanced performance with CS and MK [51]. This research advances knowledge by providing a detailed understanding of how CS and MK can be effectively used in concrete to achieve sustainability goals. It fills a previously unconsidered gap by offering a systematic approach to optimizing material proportions and assessing their environmental impact, thus paving the way for more eco-friendly construction practices worldwide [52].

## 2 Experimental methods

### 2.1 Test materials

The binding material used is the Ultratech 53 Grade of OPC, and the corresponding supplementary cementitious material utilized in this investigation is MK. As reported by IS 269 [53] guidelines, the material complies with multiple standard tests. Table 1 shows the chemical composition of cement and MK, and Figure 2 illustrates the X-ray diffraction of MK. Cement has a specific gravity of 3.15, compared to 2.6 for MK. The combined quantities of  $SiO_2$ ,  $Al_2O_3$ , and  $Fe_2O_3$  were greater than the required minimum of 70. Designed for applications that demand significant water reduction and extended workability, Viscoflux 5507 is a

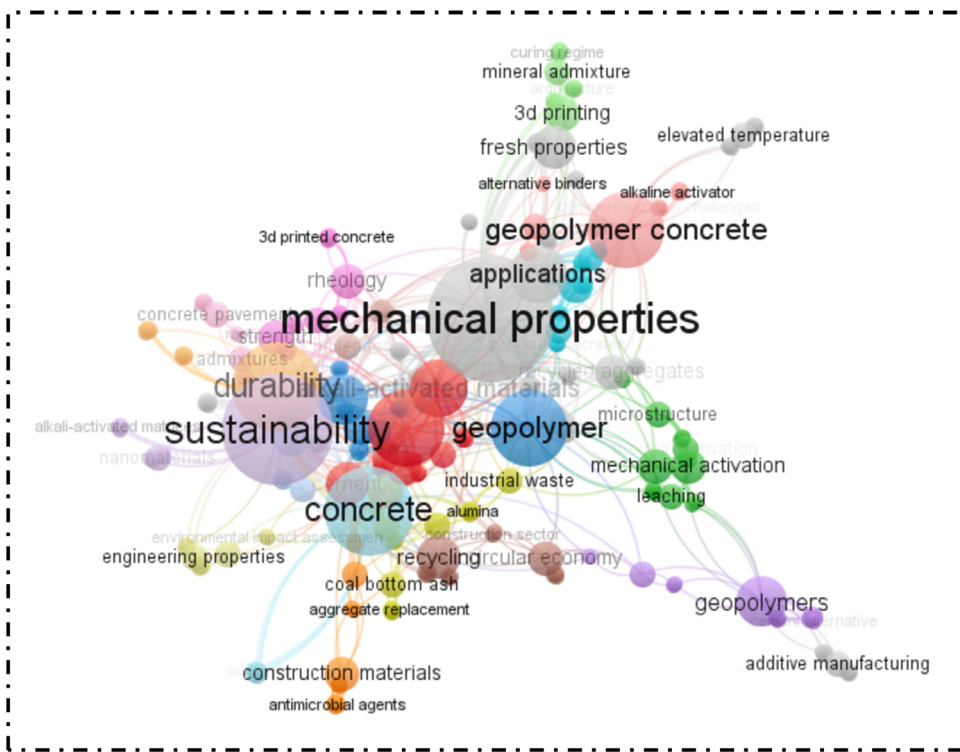


**Figure 1:** Cluster diagram showing the relationship of mechanical properties.

**Table 1:** Chemical properties of cement and MK

Component	Cement	MK
SiO <sub>2</sub>	18.89	54.899
K <sub>2</sub> O	1.14	0.162
CaO	62.37	0.279
MgO	0.99	0.914
P <sub>2</sub> O <sub>5</sub>	0.12	0.03
Fe <sub>2</sub> O <sub>3</sub>	3.83	0.799
Al <sub>2</sub> O <sub>3</sub>	4.24	38.145
Na <sub>2</sub> O	0.12	0.01
TiO <sub>2</sub>	0.30	2.061

high-performance superplasticizer. In this case, 1.0% of the cement's weight was used as a plasticizer in the mixture.

Locally sourced coarse aggregates with nominal sizes of 10 and 20 mm were used in equal proportions of 50% each. The specific gravity, water absorption, and fineness modulus are conducted as per IS 2386 Part III [54].

NS that was readily available locally was utilized in concrete mixtures that conformed to IS 383 [55]. It is classified into four zones by the IS 383 [55] based on the particle size determined by sieve analysis; Zone II was found to be the case for this particular sand. The physical and chemical properties of NS are shown in Table 2. The X-ray diffraction of CS is shown in Figure 3.

CS from Birla Copper in Gujarat is utilized in this study. The material is heavier due to its high specific gravity. Table 2 shows the physical and chemical properties of NS compared to CS. Figure 4 shows the particle size distribution for NS and CS.

## 2.2 Test procedure

A total of eight concrete mixes were used for this experimental work and are shown in Table 3. The study involved preparing, casting, and testing different mixes to determine the mechanical properties using different proportions of CS and MK. The curing of specimens was carried out for 7, 14, 28, and 56 days to determine the mechanical properties of the concrete. The experimental work was divided into two phases: the first phase tested CS as a partial substitute for fine aggregate in amounts from 10 to 40%, increasing by 10% increments.

The second phase involved adding MK as a partial replacement for cement at 5, 10, and 15%, along with 30% CS replacing sand. The optimum percentage obtained for CS as a part switch of sand is obtained in phase I. The concrete mixes blended with MK and CS are prepared, cast, and tested for strength. The quantity of all the materials is shown in

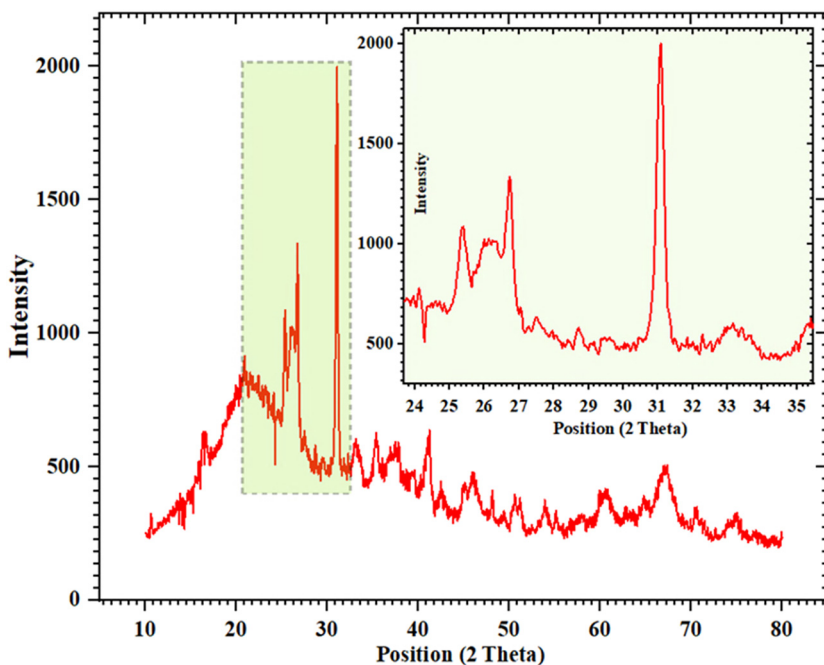


Figure 2: X-ray diffraction of MK.

Table 2: Physical properties of coarse and fine aggregate

Component	NS	CS	Coarse aggregate
Specific gravity (g/cc)	2.64	3.31	2.89
Water absorption (%)	1.06	0.87	0.89
Fineness modulus	2.84	2.86	6.93
Bulk of sand (%)	28	—	—
Chemical properties of fine aggregates			
SiO <sub>2</sub>	73.79	20.328	—
K <sub>2</sub> O	3.46	0.723	—
CaO	1.79	2.721	—
MgO	0.47	0.859	—
P <sub>2</sub> O <sub>5</sub>	0.13	0.1	—
Fe <sub>2</sub> O <sub>3</sub>	2.69	64.733	—
Al <sub>2</sub> O <sub>3</sub>	15.39	3.076	—
Na <sub>2</sub> O	0.59	0.425	—
TiO <sub>2</sub>	0.34	0.391	—

Table 4 for all the mixes. The methodology adopted in this research work is also depicted in Figure 5.

In the initial state, the workability test was carried out as per IS 1199 [56]. Workability of the fresh concrete was measured using the slump cone test.

To evaluate the mechanical properties of the hardened concrete, strength tests were conducted on both the control and developed concrete, including tests for compressive strength, split tensile strength, and flexural strength [57].

Following IS Code 516 [58], compressive strength testing was carried out on cubes of size 150 mm ×

150 mm × 150 mm at 7, 14, 28, and 56 days of moist curing. The tests were performed using a 2,000 kN capacity compression testing machine, as depicted in Figure 6a. The average of strengths for three specimens is considered the strength of the concrete mix.

The flexural strength of concrete was evaluated as per IS516 [58] on the beam specimen of size 100 mm × 100 mm × 500 mm. The specimens were extracted from the curing tank at 28 and 56 days of moist curing and tested, as illustrated in Figure 6b.

The split tensile strength of concrete was conducted as per IS 5816 [59] on the cylindrical specimens, measuring 150 mm in diameter and 300 mm in height, at 28 and 56 days of moist curing. A 2,000 kN capacity compression testing machine was used for the tests, as demonstrated in Figure 6c.

For durability assessment, the rapid chloride permeability test was conducted as per ASTM C1202 [60], as shown in Figure 6d and 6e. The test specimen of cubes was tested for resistance against chloride ion penetration after 28 and 56 days of moist curing in water.

### 3 Results and discussion

#### 3.1 Workability

The results indicate that the workability of the mix CS40 is a maximum of 120 mm as compared to the CC mix, *i.e.*,

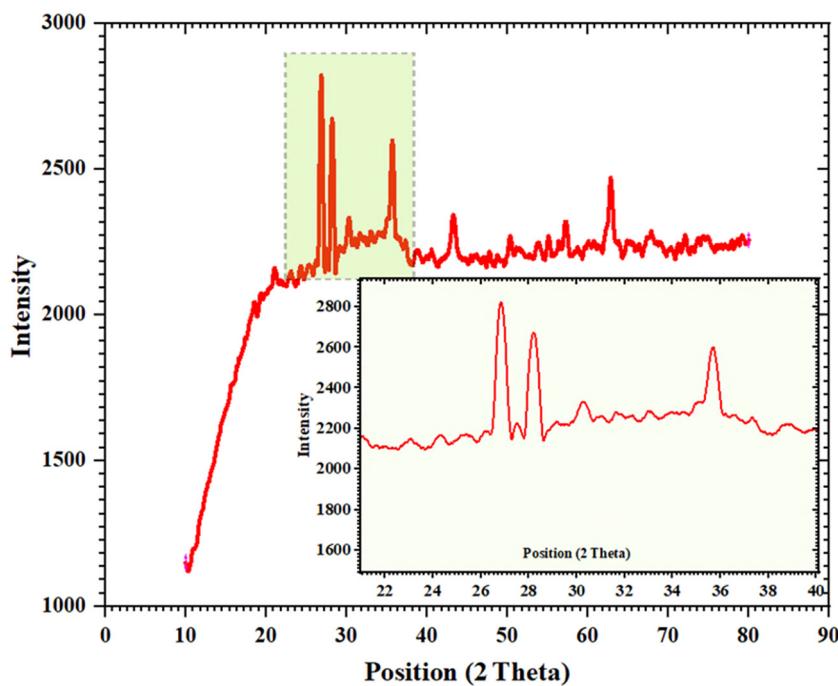


**Figure 3:** X-ray diffraction of CS.

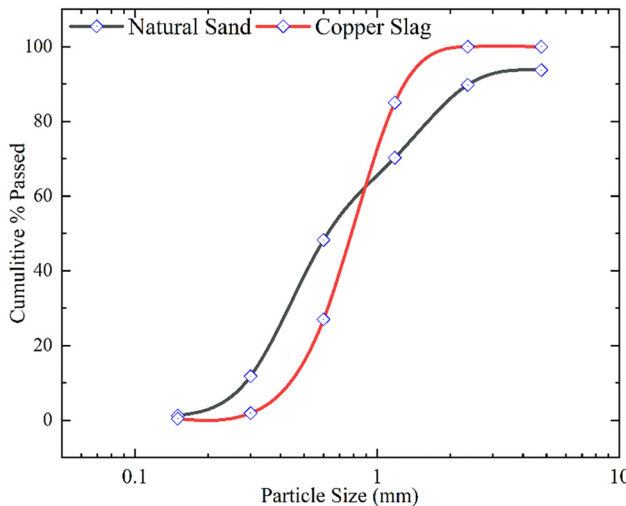


**Figure 4:** Particle size distribution of NS and CS.

90 mm, as presented in Table 5. The increase can be explained by the excess free water remaining post-absorption and hydration, as CS's glassy or smooth surface results in a lower water absorption rate compared to NS [61,62]. The mix MK15CS30 has a minimum workability of 91 mm, as shown in Figure 7; however, the workability progressively declines due to the addition of MK, as presented in Table 5.

**Table 3:** Percentage of constituents of concrete for different mixes

S.N	Mix	Proportion				
		Cement		Fine aggregate		
		OPC	MK	NS	CS	CA
1	CC	100	0	100	—	100
2	CS10	100	0	90	10	100
3	CS20	100	0	80	20	100
4	CS30	100	0	70	30	100
5	CS40	100	0	60	40	100
6	MK5CS30	95	5	70	30	100
7	MK10CS30	90	10	70	30	100
8	MK15CS30	85	15	70	30	100

OPC: Ordinary Portland cement; NS: natural sand; CA: coarse aggregate.

### 3.2 Density

The increase in the density of the concrete mix with increasing CS content is illustrated in Figure 7. This is because CS has a specific gravity of 3.31, which is greater than that of NS(2.64). Incorporating MK into the concrete mix as a cement reduces the density of concrete, as shown in Table 5. The study found that the workability of concrete increases with higher CS content, while the addition of MK as a cement replacement decreases workability. This is

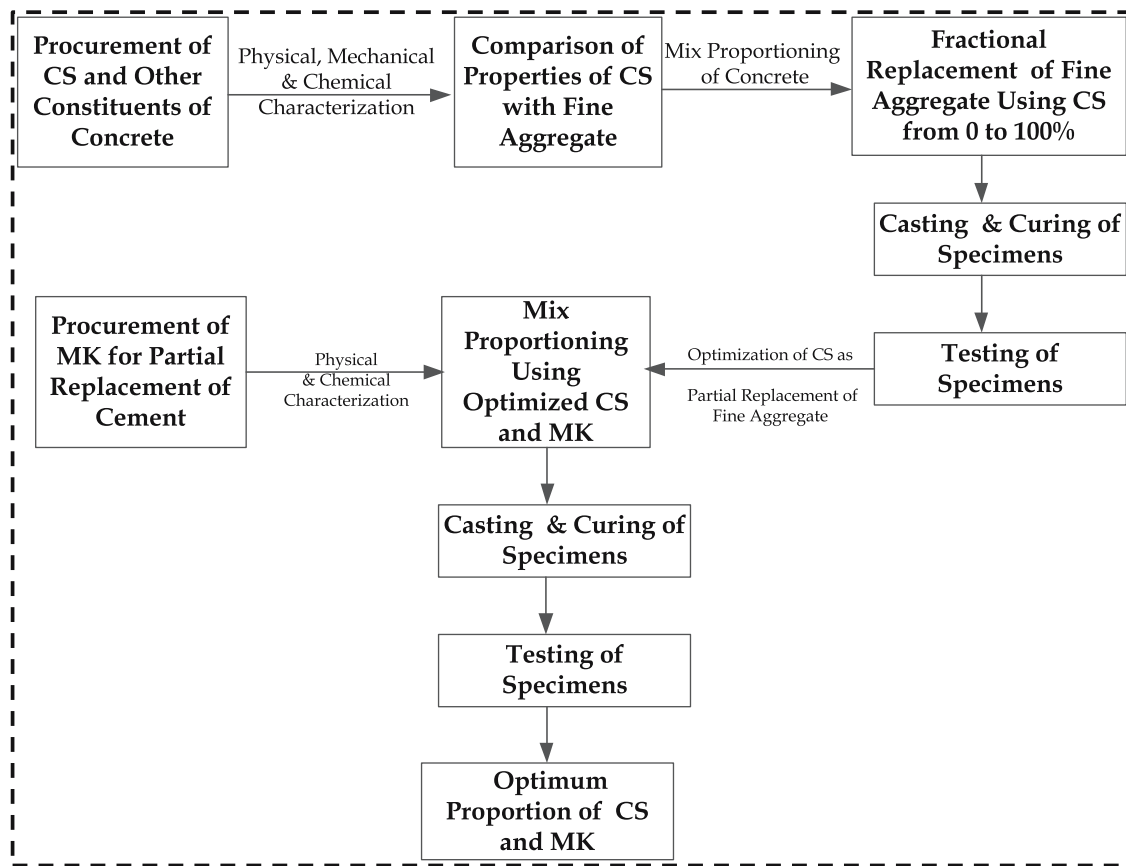
**Table 4:** Quantity of constituents of concrete (in  $\text{kg}\cdot\text{m}^{-3}$ )

S.N	Mix	Cement ( $\text{kg}\cdot\text{m}^{-3}$ )		Fine aggregate ( $\text{kg}\cdot\text{m}^{-3}$ )		CA	Super plasticizer	W/C ratio
		OPC	MK	NS	CS			
1	CC	350	—	701.18	—	1368.17	3.50	0.45
2	CS10	350	—	631.06	88.08	1368.17	3.50	0.45
3	CS20	350	—	560.94	176.16	1368.17	3.50	0.45
4	CS30	350	—	490.83	264.25	1368.17	3.50	0.45
5	CS40	350	—	420.71	352.33	1368.17	3.50	0.45
6	MK5CS30	332.5	17.5	490.05	263.83	1366.02	3.50	0.45
7	MK10CS30	315.0	35.0	489.28	263.41	1363.86	3.50	0.45
8	MK15CS30	297.5	52.5	488.51	263.00	1361.70	3.50	0.45

attributed to the smoother texture of CS, which enhances workability, but excessive CS can lead to bleeding and segregation if used beyond 50% replacement. The density of concrete increases with more CS but decreases with MK, indicating a trade-off between workability and density when using these materials.

### 3.3 Compressive strength

Figure 8 illustrates the compressive strength of concrete made with CS and MK. The results from the compressive strength test show that the CS30 mix in the first phase outperforms all other mixes. The highest compressive strength

**Figure 5:** Methodology for the work performed.

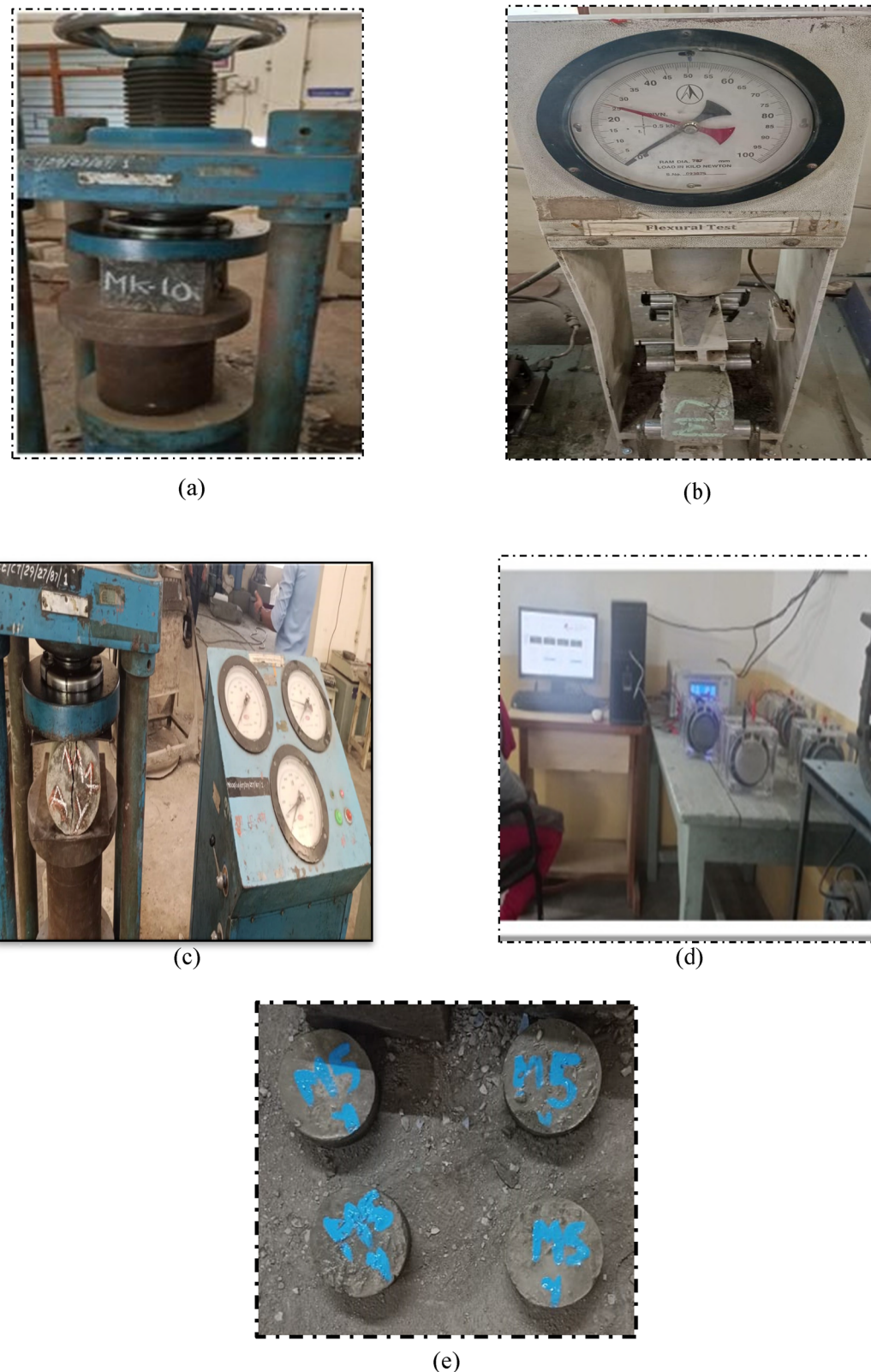


**Figure 6:** Testing of specimens. (a) Cube specimen, (b) beam specimen, (c) cylindrical specimen, (d) RCPT testing, and (e) RCPT specimen.

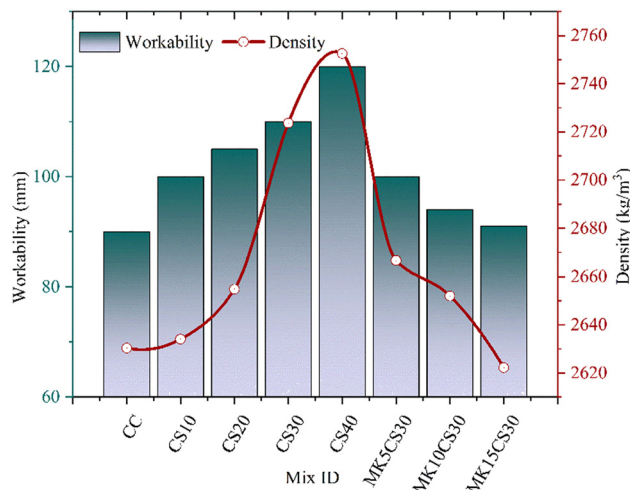
**Table 5:** Test results for 7, 14, 28, and 56 days curing

S.N	Mix	Slump (mm)	Compressive strength (N·mm <sup>-2</sup> )				Flexural strength (N·mm <sup>-2</sup> )		Split tensile strength (N·mm <sup>-2</sup> )		Density (kg·m <sup>-3</sup> )
			7	14	28	56	28	56	28	56	
1	CC	90	36.69	37.78	39.53	41.22	7.85	8.11	2.86	2.91	2630.37
2	CS10	100	39.80	42.67	46.23	48.76	8.90	9.28	2.96	3.03	2634.07
3	CS20	105	41.78	44.44	48.55	50.92	9.24	9.88	3.15	3.24	2654.81
4	CS30	110	43.56	45.78	50.33	53.16	9.52	10.1	3.46	3.55	2723.70
5	CS40	120	37.78	40.00	48.66	51.98	8.40	8.87	3.25	3.43	2752.59
6	MK5CS30	100	40.22	48.41	53.33	56.43	9.60	10.15	3.54	3.66	2666.67
7	MK10CS30	94	41.56	49.44	57.78	61.43	10.2	10.65	3.70	3.81	2652.00
8	MK15CS30	91	40.11	48.54	56.89	60.11	9.80	10.45	3.64	3.75	2622.22

values for CS30 are 50.33 N·mm<sup>-2</sup> at 28 days and 53.16 N·mm<sup>-2</sup> at 56 days, showing an increase of 27.32 and 28.97%, respectively. This improvement can be attributed to the higher iron oxide (Fe<sub>2</sub>O<sub>3</sub>) content and the inherent toughness of CS.

All of the mixes containing MK show higher compressive strength as compared to the concrete made only with CS. The MK10CS30 mix outperformed all the other mixes, as it exhibited higher compressive strengths of 57.78 and 61.43 N·mm<sup>-2</sup> with an increase of 46.16 and 49.03% at 28 and 56 days, respectively. Also, MK15CS30 shows higher strengths of 43.91 and 45.83% at 28 and 56 days, as compared to the CC mix.

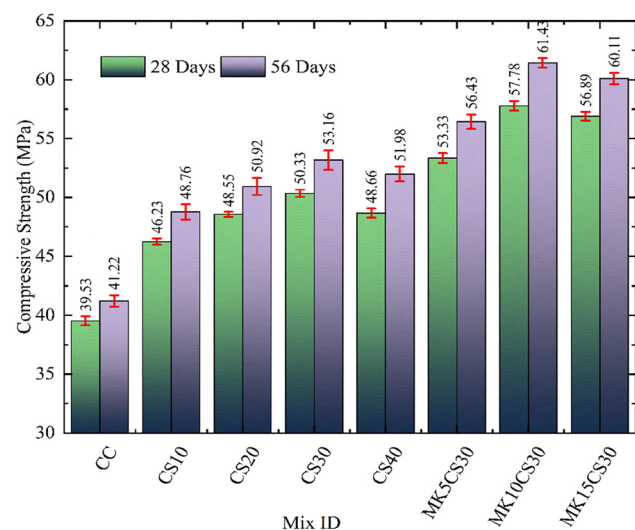
Mixes CS10, CS20, CS30, CS40, MK5CS30, MK10CS30, and MK15CS30 show an increase in compressive strength by 16.95, 22.82, 27.32, 23.10, 34.92, 46.16, and 43.91% at 28 days and 18.29, 23.53, 28.97, 26.10, 36.90, 49.03, and 45.83% at 56 days, respectively, with respect to CC. This suggests that the combination of MK and CS optimizes the compressive strength of concrete.

**Figure 7:** Density and workability for different concrete mixes.

### 3.4 Flexural strength

The flexural tensile strength of CS10, CS20, CS30, and CS40 increases by 13.38, 17.71, 21.27, and 7.01% at 28 days and 14.43, 21.82, 24.54, and 9.37%, respectively, with respect to the CC mix in the first phase of research. Mix CS30 exhibited higher flexural strengths of 9.52 and 10.1 N·mm<sup>-2</sup>, as shown in Figure 9, with an increase of 21.27 and 24.54% at 28 and 56 days. The highest flexural strengths of 10.2 and 10.65 N·mm<sup>-2</sup> were achieved for MK10CS30 with an increase of 29.94 and 31.32%, as compared to the CC mix.

The other MK blended concrete samples, *i.e.*, MK5CS30, MK10CS30, and MK15CS30, show the maximum flexural strengths of 22.29, 29.94, and 24.84% at 28 days, and 25.15, 31.32, 28.85% at 56 days, respectively, as associated with CC. This indicates that MK and CS not only improve the compressive strength but also enhance the tensile and flexural properties of the concrete.

**Figure 8:** Variation in the compressive strength for concrete mixes.

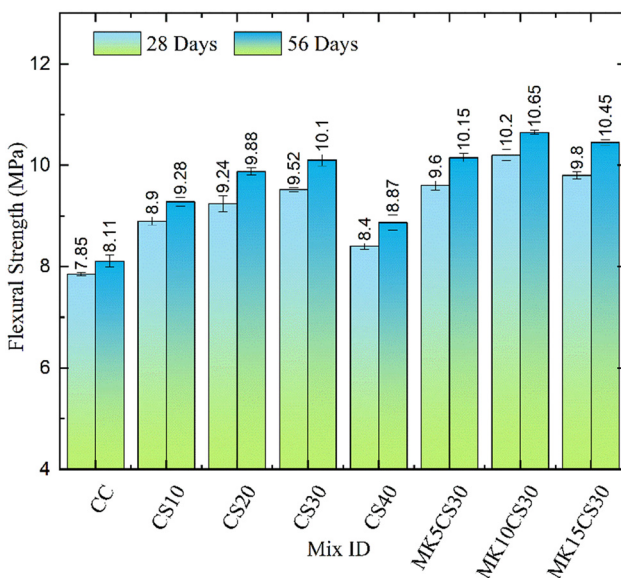


Figure 9: Variation in the flexural strength for concrete mixes.

### 3.5 Split tensile strength

The splitting tensile strength test results in the first phase indicated that the strengths of concrete mix CS30 are 3.46 and  $3.55 \text{ N}\cdot\text{mm}^{-2}$ , which are higher by 20.98 and 21.99% at 28 and 56 days, respectively, as compared to CC, as shown in Figure 10.

In the second phase of research, the flexural strengths for MK5CS30, MK10CS30, and MK15CS30 increase by 23.73, 29.37, and 27.27% at 28 days and 25.77, 30.93%, and 28.87 at 56 days, respectively. The concrete mix MK10CS30

outperformed among all the other mixes as it exhibited maximum strengths of  $3.7 \text{ and } 3.81 \text{ N}\cdot\text{mm}^{-2}$  with an increase of 29.37 and 30.93% at 28 and 56 days, respectively. The incorporation of MK as a fractional substitution of cement induced a remarkable strength to the concrete. Hence, the splitting tensile strength of the modified concrete mixes is enhanced compared to the control concrete.

### 3.6 Rapid chloride ion penetration test

The durability of concrete is assessed by using the rapid chloride ion penetration test on the concrete cube of  $100 \text{ mm} \times 50 \text{ mm}$ , as shown in Figure 6e. The Coulomb's charge for the CC mix was found to be 2133.45 and 1880.87 on the 28th and 56th day, showing moderate penetration as per ASTM C1202. The charge passed for CS30 showed higher values than the control concrete, *i.e.*, 3512.07 and 3220.34 at 28 and 56 days, respectively, as shown in Figure 11, but within the limits as per ASTM C1202. Due to the addition of MK in the second phase, *i.e.*, for MK5CS30, MK10CS30, and MK15CS30, the Coulomb charge reduces as compared to the CC and CS30 mixes. The resistance against chloride ion penetration for the MK10CS30 and MK15CS30 mixes was found to be at a lower level as per ASTM C1202. The Coulomb charges for this mix are 1520.14 and 1390.36 at 56 days, respectively, as shown in Figure 11. This shows remarkably lower permeability than the CC and CS30 mixes. MK reduced the chloride ion permeability, indicating lower permeability of the MK-CS concrete. The addition of MK reduces the pores of concrete and makes the concrete impermeable.

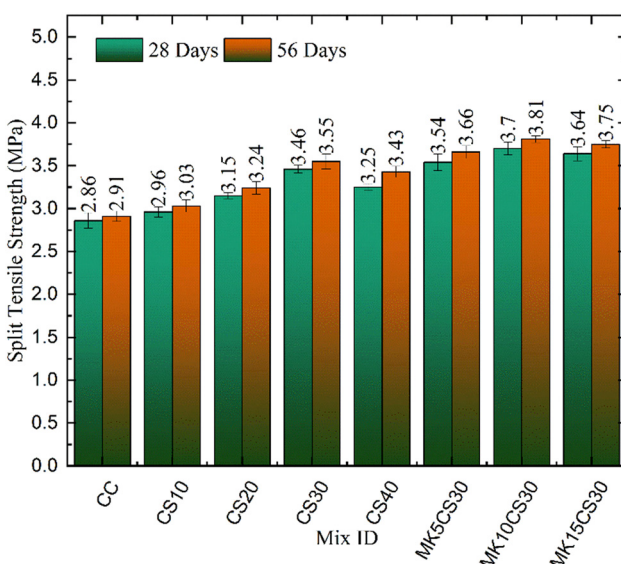


Figure 10: Variation in the splitting tensile strength for concrete mixes.

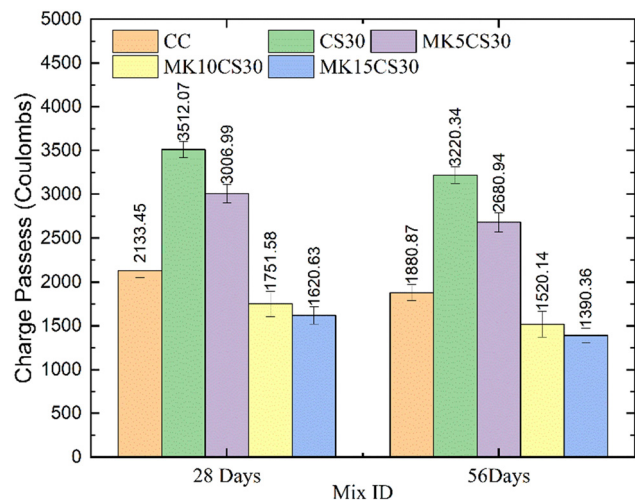
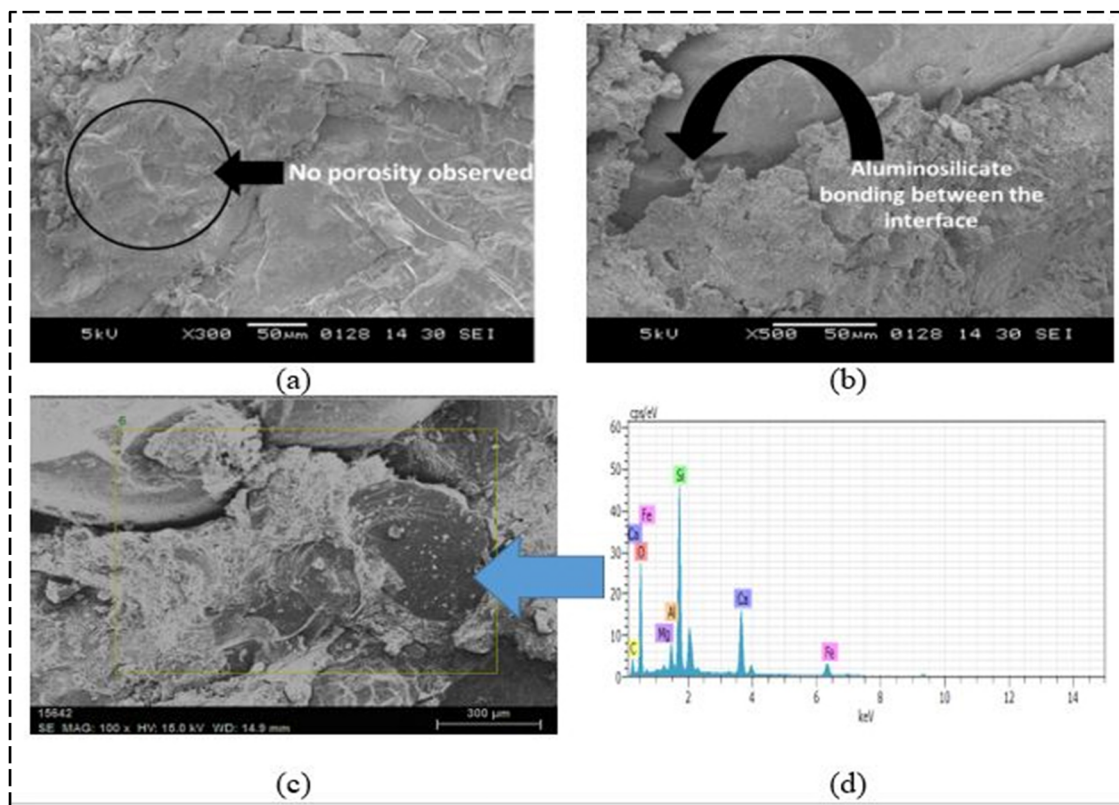


Figure 11: Variation in charge passes for different concrete mixes.



**Figure 12:** Microstructural analysis of the concrete with 10% MK and 30% CS. (a) No porosity observed, (b) aluminosilicate bonding between interface, (c) presence of Ca and Al at the interface, and (d) energy dispersive spectrograph of concrete.

### 3.7 Microstructural analysis

After observing promising results in the strength and durability of MK10CS30, an SEM investigation was conducted. The SEM analysis confirmed a denser microstructure, clearly illustrating the benefit of CS inclusion. Reduced porosity, as evidenced by the SEM microstructure in Figure 12(a), minimizes pathways for harmful substances, thereby enhancing durability by lowering the potential for corrosion, cracking, and deterioration. Additionally, Figure 12(b) shows aluminosilicate bonding at the interface. In this study, supplementary

cementitious materials like MK, which are rich in aluminosilicate, were added. These materials undergo pozzolanic reactions with CH, leading to the formation of the additional C-S-H gel. This gel contributes to the overall strength and durability of concrete. In addition, the CS added to the concrete enriches the bonding by facilitating the formation of calcium aluminosilicate bonding, which can be ascertained through the energy dispersive spectrograph shown in Figure 12(c) and (d), which indicates the presence of Ca and Al at the interface. Thus, the mix MK10CS30 has proved beneficial, contributing to the strength of the material.

**Table 6:** Responses provided for the MK and CS factors

S.N	Factor 1, MK (%)	Factor 2, CS (%)	Response 1, compressive strength (MPa)	Response 2, flexural strength (MPa)
1	0	0	39.53	7.85
2	0	10	46.23	8.90
3	0	20	48.55	9.24
4	0	30	50.33	9.52
5	0	40	48.66	8.40
6	5	30	53.33	9.60
7	10	30	57.77	10.20
8	15	30	56.88	9.80

### 3.8 Optimization of MK and CS using RSM

Considering the results obtained for the mechanical properties of concrete using MK and CS, the optimization of

**Table 7:** Regression equations for the various parameter levels

Responses	Regression model	R <sup>2</sup>	Eq.
Compressive strength (MPa)	$=54.81 + 3.61A + 4.40B + 0.00004B^2 - 2.18A^2 - 4.84B^2$	0.9880	(1)
Flexural strength (MPa)	$=10.09 + 0.3108A + 0.3309B + 0.00004B^2 - 0.3884A^2 - 1.24B^2$	0.9552	(2)

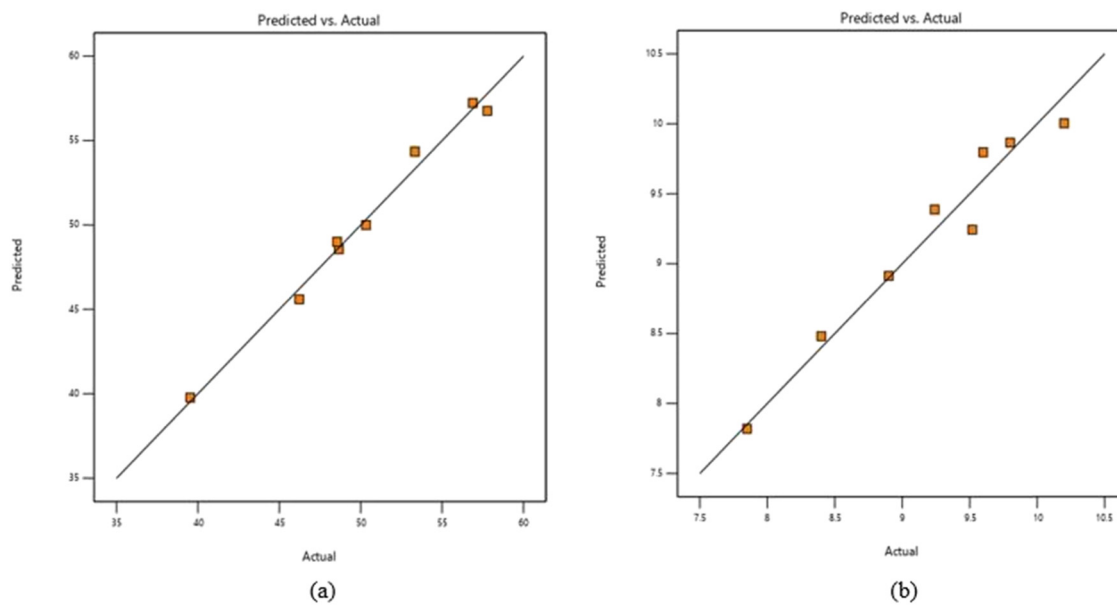


**Figure 13:** Predicted and actual (a) compressive strength and (b) flexural strength.

these elements is conducted using the Central Composite Design process in RSM [63]. A quadratic model is fitted for predicting the optimization. A statistical model of analysis is conducted to optimize the quantities of CS and MK in concrete by obtaining the maximum compressive and flexural strengths for the tailored concrete. Table 6 presents the responses recorded for the experiment. The regression equations obtained from the analysis of variance are shown in Table 7.

The equation, expressed in terms of coded factors, can be used to predict the response for specific levels of each factor. Here,  $A$  represents the percentage of MK, while  $B$  indicates the percentage of CS. The predicted versus actual compressive and flexural strengths are shown in Figure 13. An  $F$ -value analysis was performed to determine the optimal outcome [15,64]. The  $F$ -values obtained for this analysis were 61.57 and 15.98 for compressive and flexural strengths, respectively. The  $P$ -values were less than 0.05,

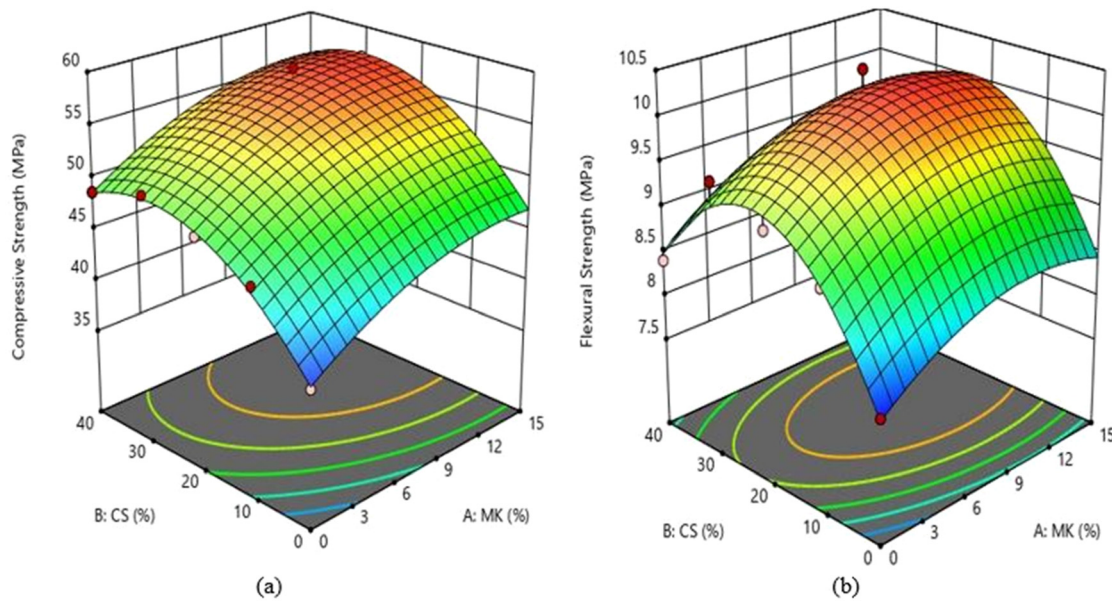


**Figure 14:** Three-dimensional surface representation for (a) compressive strength and (b) flexural strength.

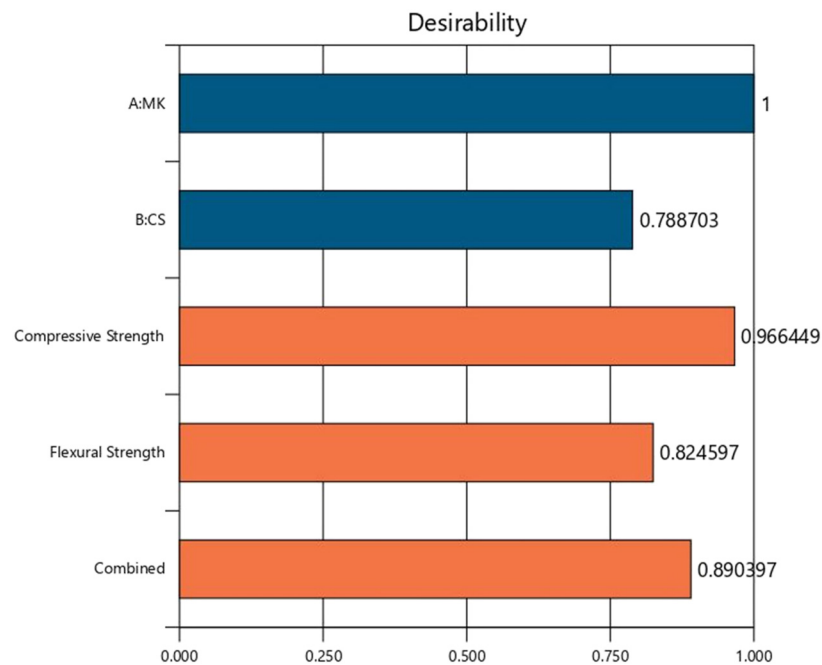


**Figure 15:** Desirability chart for factors and responses considered in the study.

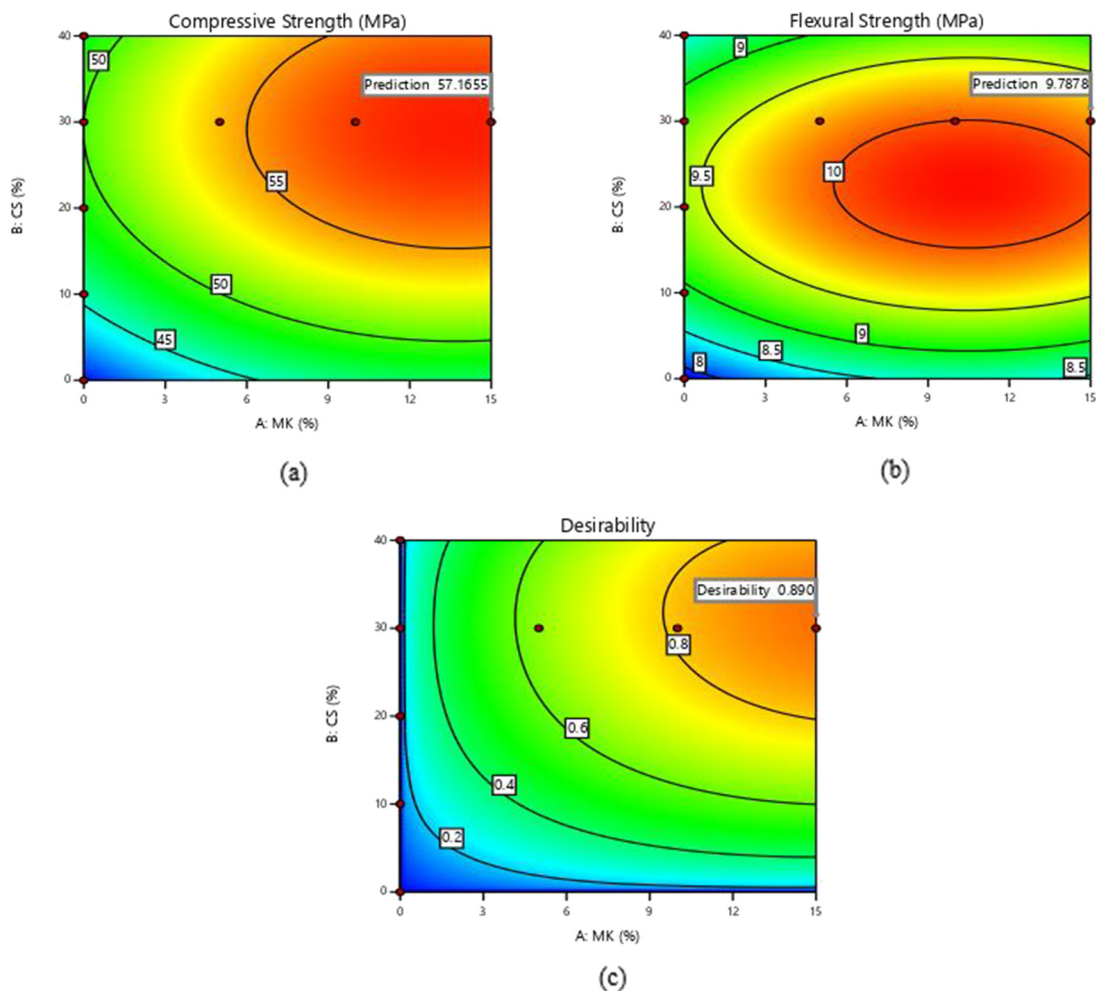


**Figure 16:** Contour surface plots for (a) compressive strength, (b) flexural strength, and (c) desirability of the model.

which indicates that the models were significant. The experimental findings and predicted values from the RSM model showed a strong correlation as  $R$  squared ( $R^2$ ) values obtained were 0.9880 and 0.9552 for compressive and flexural strengths, respectively.

As depicted in Figure 14, a three-dimensional surface plot was employed to describe the optimization and verification of the models. The study extensively explored the complex relationship between MK and CS levels and the concrete's mechanical properties, with a focus on compressive and flexural strengths. The desirability function was used in the optimization process to provide a quantitative method for determining the upper and lower limits of these strengths, enabling the determination of the desirability level. The study reached a combined desirability score of 0.8903, as shown in Figure 15. The optimal strengths were found at 15% MK and 31.533% CS. The contour plots used for optimization are shown in Figure 16.

## 4 Conclusion

- Concrete's workability increases with higher CS content, but adding MK as a replacement for cement decreases workability.
- With a compressive strength of roughly  $50.33 \text{ N} \cdot \text{mm}^{-2}$ , the CS30 mix outperformed the control mixture, which had a value of  $39.53 \text{ N} \cdot \text{mm}^{-2}$ . This indicates an almost 27.32% increase in strength compared to the control mix. However, the lowest compressive strength was found in CS80 and CS100 with greater CS concentrations.
- The highest compressive strengths achieved for MK10CS30 were 57.78 and  $63.13 \text{ N} \cdot \text{mm}^{-2}$  at 28 and 56 days, respectively, enhancing the strength by 46.16 and 49.02% as compared to the CC mix.
- The maximum split tensile strength was found for MK10CS30 at an increment of 29.37 and 30.93% at 28 and 56 days, respectively.
- For MK10CS30, the highest flexural strengths of 10.2 and  $10.65 \text{ N} \cdot \text{mm}^{-2}$  with an increase of 29.94 and 31.32% at 28 and 56 days, respectively.
- All the mixes containing MK showed higher strength as compared to other mixes.
- Concrete becomes denser with an increased amount of CS, while incorporating MK leads to a reduction in density.
- According to the RCPT results, concrete blended with slag and MK greatly densified the matrix, which reduces permeability and enhances the strength as seen in compression and flexural strengths. It was found that MK

concrete exhibits a significantly higher resistance to chloride ion penetration.

- Moreover, the SEM micrograph of MK10CS30 demonstrated a homogeneous and dense structure of the C–S–H gel.
- The RSM used in the study revealed that MK can be used as a partial replacement of cement up to 15% and the fine aggregates can be exchanged up to 31.533% using CS.
- Finally, this study shows that the use of CS as a partial replacement of NS has some limitations, as the texture of CS is smoother, and hence it makes concrete more workable, and there might be the chances of bleeding and segregation if the partial replacement is beyond 50%. However, the utilization of MK is itself challenging, as the high-performance MK is not available in all parts of the globe; in addition, water demand and early age shrinkage can be the concerning factors for MK as a fractional switch of cement. Further research for life cycle assessment and carbon footprint emission can be carried out for utilizing the MK and CS as partial replacements of cement and NS to make construction activity sustainable.

Overall, this research provides significant insights into the use of alternative materials in concrete, offering a pathway to more sustainable and efficient construction practices, offering a practical solution to environmental challenges while potentially improving concrete performance and economics in the construction industry.

**Acknowledgments:** The authors would like to acknowledge the Ongoing Research Funding program (ORF-2025-473), King Saud University, Riyadh, Saudi Arabia, and Dirección de Investigación de la Universidad Católica de la Santísima Concepción, Concepción, Chile.

**Funding information:** The authors would like to acknowledge the support provided by the Ongoing Research Funding program (ORF-2025-473), King Saud University, Riyadh, Saudi Arabia, Dirección de Investigación de la Universidad Católica de la Santísima Concepción, Concepción, Chile, and Departamento de Ciencias de la Construcción, Facultad de Ciencias de la Construcción Ordenamiento Territorial, Universidad Tecnológica Metropolitana, Santiago.

**Author contributions:** Amruta Yadav – conceptualization, methodology, software, validation, formal analysis, investigation, data curation, writing – original draft, writing – review and editing, and resources. Ajay Gajbhiye – investigation, data curation, writing – original draft, writing –

review and editing, resources, and visualization. Dhiraj Agrawal – conceptualization, methodology, software, validation, formal analysis, investigation, data curation, writing – original draft, writing – review and editing, resources, visualization, supervision, and project administration. Khalid Ansari – conceptualization, methodology, software, validation, formal analysis, investigation, data curation, writing – original draft, writing – review and editing, resources, visualization, supervision, and project administration. Abdullah H. Alsabhan – conceptualization, methodology, software, validation, formal analysis, investigation, data curation, writing – original draft, writing – review and editing, resources, and funding acquisition. Krishna Prakash Arunachalam – software, validation, formal analysis, investigation, data curation, writing – original draft, and writing – review and editing. Siva Avudaiappan – investigation, data curation, writing – review and editing, resources, visualization, and funding acquisition. Nelson Maureira-Carsalade – investigation, data curation, writing – review and editing, resources, visualization, and funding acquisition. Osamah J. Alsareji – software, validation, formal analysis, investigation, data curation, writing – original draft, writing – review and editing, and resources. All authors have accepted responsibility for the entire content of this manuscript and approved its submission.

**Conflict of interest:** The authors state no conflict of interest.

**Data availability statement:** The datasets generated and/or analyzed during the current study are available from the corresponding author on reasonable request.

## References

- [1] Negm, A. A., A. El Nemr, F. Elgabbas, and M. A. Khalaf. High and normal strength concrete using grounded vitrified clay pipe (GVCP). *Cleaner Materials*, Vol. 5, 2022, id. 100107.
- [2] Gill, P., V. S. Rathanasalam, P. Jangra, T. M. Pham, and D. K. Ashish. Mechanical and microstructural properties of fly ash-based engineered geopolymers mortar incorporating waste marble powder. *Energy, Ecology and Environment*, Vol. 9, No. 2, Springer 2024, pp. 159–174.
- [3] Agrawal, D., K. Ansari, U. Waghe, M. Goel, S. P. Raut, H. Warade, et al. Exploring the impact of pretreatment and particle size variation on properties of rubberized concrete. *Scientific Reports*, Vol. 15, No. 1, 2025, id. 11394.
- [4] Mohamed, M.A.M., F. Elgabbas, A. El-Nemr, and M. A. Khalaf. The influence of glass powder as a cement replacement material on ultra-high-performance concrete. *CERM*, Vol. 43, 2021, pp. 315–323.
- [5] El Nemr, A. M., M. A. Shawky, and M. El Khafif. The effect of mineral pigments on mechanical properties of concrete. *Journal of Civil Engineering and Construction*, Vol. 11, No. 3, 2022, pp. 139–152.
- [6] Garg, A., P. Jangra, D. Singhal, T. M. Pham, and D. K. Ashish. Durability studies on conventional concrete and slag-based geopolymers concrete in aggressive sulphate environment. *Energy, Ecology and Environment*, Vol. 9, No. 3, Springer 2024, pp. 314–330.
- [7] Ashish, D. K.. Concrete made with waste marble powder and supplementary cementitious material for sustainable development. *Journal of Cleaner Production*, Vol. 211, Elsevier 2019, pp. 716–729.
- [8] Prasittisopin, L.. Power plant waste (fly ash, bottom ash, biomass ash) management for promoting circular economy in sustainable construction: emerging economy context. *Smart and sustainable built environment*, 2024 ahead-of-p(ahead-of-print).
- [9] Gill, P., P. Jangra, and D. K. Ashish. Non-destructive prediction of strength of geopolymers concrete employing lightweight recycled aggregates and copper slag. *Energy, Ecology and Environment*, Vol. 8, No. 6, 2023, pp. 596–609.
- [10] Ameri, F., P. Shoaei, H. R. Musaei, S. A. Zareei, and C. B. Cheah. Partial replacement of copper slag with treated crumb rubber aggregates in alkali-activated slag mortar. *Construction and Building Materials*, Vol. 256, 2020, id. 119468.
- [11] Al-Jabri, K. S., M. Hisada, S. K. Al-Oraimi, and A. H. Al-Saidy. Copper slag as sand replacement for high performance concrete. *Cement and Concrete Composites*, Vol. 31, No. 7, 2009, pp. 483–488.
- [12] Arunachalam, K. P., S. Avudaiappan, N. Maureira-Carsalade, F. D. C. Garcia Filho, S. N. Monteiro, I. D. Batista, et al. Innovative use of copper mine tailing as an additive in cement mortar. *Journal of Materials Research and Technology*, Vol. 25, 2023, pp. 2261–2274.
- [13] Nagarajan, D., R. Prakash, S. Srividhya, S. Avudaiappan, P. Guindos, N. M. Carsalade, et al. Experimental and numerical investigations of laced built-up lightweight concrete encased columns subjected to cyclic axial load. *Buildings*, Vol. 13, No. 6, 2023, id. 1444.
- [14] Edwin, R. S., E. Gruyaert, and N. De Belie. Valorization of secondary copper slag as aggregate and cement replacement in ultra-high performance concrete. *Journal of Building Engineering*, Vol. 54, 2022, id. 104567.
- [15] Waghe, U., D. Agrawal, K. Ansari, M. Waghe, M. Amran, B. T. Alsulami, et al.. Enhancing eco-concrete performance through synergistic integration of sugarcane, metakaolin, and crumb rubber: Experimental investigation and response surface optimization. *Journal of Engineering Research*, Vol. 12, No. 4, 2024, pp. 645–658.
- [16] Al-Jabri, K. S., A. H. Al-Saidy, and R. Taha. Effect of copper slag as a fine aggregate on the properties of cement mortars and concrete. *Construction and Building Materials*, Vol. 25, No. 2, 2011, pp. 933–938.
- [17] Patil, M. V. and Y. D. Patil. Effect of copper slag and granite dust as sand replacement on the properties of concrete. *Materials Today: Proceedings*, Elsevier Ltd 2020, pp. 1666–1677.
- [18] Sharma, R. and R. A. Khan. Influence of copper slag and metakaolin on the durability of self compacting concrete. *Journal of Cleaner Production*, Vol. 171, Elsevier Ltd 2018, pp. 1171–1186.
- [19] Harikaran, M., S. Gokulakannan, A. Loganathan, R. D. Chandiran, M. Ajith, and V. Dhanasekar. Metakaolin cement concrete evaluation using industrial by-products as fine aggregate. *Materials Today: Proceedings*, 2023. Doi: 10.1016/j.matpr.2023.04.586
- [20] Karatas, M., M. Dener, M. Mohabbi, and A. Benli. A study on the compressive strength and microstructure characteristic of alkali-

activated metakaolin cement. *Matéria (Rio de Janeiro)*, Vol. 24, SciELO Brasil 2019, id. e12507.

[21] Bheel, N., P. Awoyeria, I. A. Shar, S. A. Abbasi, S. H. Khahro, and K. P. Arunachalam. Synergic effect of millet husk ash and wheat straw ash on the fresh and hardened properties of Metakaolin-based self-compacting geopolymer concrete. *Case Studies in Construction Materials*, Vol. 15, 2021, id. e00729.

[22] Zhang, M. H. and V. M. Malhotra. Characteristics of a thermally activated aluminosilicate pozzolanic material and its use in concrete. *Cement and Concrete Research*, Vol. 25, No. 8, 1995, pp. 1713–1725.

[23] Paiva, H., A. Velosa, P. Cachim, and V. M. Ferreira. Effect of metakaolin dispersion on the fresh and hardened state properties of concrete. *Cement and Concrete Research*, Vol. 42, No. 4, 2012, pp. 607–612.

[24] Arslan, S., A. Öz, A. Benli, B. Bayrak, G. Kaplan, and A. C. Aydin. Sustainable use of silica fume and metakaolin in slag/fly ash-based self-compacting geopolymer composites: Fresh, physico-mechanical and durability properties. *Sustainable Chemistry and Pharmacy*, Vol. 38, Elsevier 2024, id. 101512.

[25] Zhang, Q., B. Liu, Z. Sun, Q. Li, S. Wang, X. Lu, et al. Preparation and hydration process of copper slag-granulated blast furnace slag-cement composites. *Construction and Building Materials*, Vol. 421, 2024, id. 135717.

[26] Win, T., T. Buasiri, W. Pansuk, and L. Prasittisopin. Effects of combinations of limestone powder and metakaolin on mortar compressive strength development. *Suranaree Journal of Science and Technology*, Vol. 30, 2023, id. 30148.

[27] Avudaiappan, S., P. Cendoya, K. P. Arunachalam, N. Maureira-Carsalade, C. Canales, M. Amran, et al. Innovative use of single-use face mask fibers for the production of a sustainable cement mortar. *Journal of Composites Science*, Vol. 7, No. 6, 2023, id. 214.

[28] Rekha, M. S., S. R. Sumathy, K. P. Arunachalam, S. Avudaiappan, M. Abbas, and D. B. Fernande. Effects of alkaline concentration on workability and strength properties of ambient cured green geopolymer concrete. *Asian Journal of Civil Engineering*, Vol. 25, No. 6, 2024, pp. 4893–4910.

[29] Samatha, B., C. A. C. Cardenas, S. M. Ahmed, S. Avudaiappan, L. P. D Badilla, T. Marzialetti, et al. Experimental study of nanosilica based concrete with nano silica gel. In *International Conference on the Mechanical Behaviour of Materials*, Springer Nature Switzerland, Cham, 2023, pp. 315–330.

[30] Patil, A. V., V. Jayale, K. P. Arunachalam, K. S. Ansari, S. Avudaiappan, D. Agrawal, et al. Performance analysis of self-compacting concrete with use of artificial aggregate and partial replacement of cement by fly ash. *Buildings*, Vol. 14, No. 1, 2024, id. 143.

[31] San Nicolas, R., M. Cyr, and G. Escadeillas. Performance-based approach to durability of concrete containing flash-calcined metakaolin as cement replacement. *Construction and Building Materials*, Vol. 55, 2014, pp. 313–322.

[32] Nainwal, A., P. K. Emani, M. C. Shah, A. Negi, V. Kumar, and P. Negi. The influence of Metakaolin on the copper slag substituted concrete with the fine aggregate of Beas river. *Materials Today: Proceedings*, Vol. 46, 2021, pp. 10425–10432.

[33] Bayraktar, O. Y., A. Benli, B. Bodur, A. Öz, and G. Kaplan. Performance assessment and cost analysis of slag/metakaolin based rubberized semi-lightweight geopolymers with perlite aggregate: Sustainable reuse of waste tires. *Construction and Building Materials*, Vol. 411, Elsevier 2024, id. 134655.

[34] Zheng, X., J. Pan, S. Easa, T. Fu, H. Liu, W. Liu, et al. Utilization of copper slag waste in alkali-activated metakaolin pervious concrete. *Journal of Building Engineering*, Vol. 76, 2023, id. 107246.

[35] Zalnezhad, A., S. A. Hosseini, R. Shirinabadi, and M. E. Korandeh. Feasibility of using copper slag as natural aggregate replacement in microsurfacing for quality enhancement: Microscopic and mechanical analysis. *Construction and Building Materials*, Vol. 354, 2022, id. 129175.

[36] Ashish, D. K. and S. K. Verma. Determination of optimum mixture design method for self-compacting concrete: Validation of method with experimental results. *Construction and Building Materials*, Vol. 217, Elsevier 2019, pp. 664–678.

[37] Ezzedine El Dandachy, M., L. Hassoun, A. El-Mir, and J. M. Khatib. Effect of elevated temperatures on compressive strength, ultrasonic pulse velocity, and transfer properties of metakaolin-based geopolymer mortars. *Buildings*, Vol. 14, No. 7, MDPI 2024, id. 2126.

[38] Boakye, K., M. Khorami, M. Saidani, E. Ganjian, A. Dunster, M. Tyrer, et al. Influence of calcining temperature on the mineralogical and mechanical performance of calcined impure kaolinitic clays in portland cement mortars. *Journal of Materials in Civil Engineering, American Society of Civil Engineers*, Vol. 36, No. 4, 2024, id. 4024040.

[39] Kanagaraj, B., N. Anand, D. Andrushia, M. E. Mathews, J. Alengaram, P. Arulraj, et al. Mechanical properties and microstructure characteristics of self-compacting concrete with different admixtures exposed to elevated temperatures. *Jordan Journal of Civil Engineering*, Vol. 17, 2023, pp. 1–9.

[40] Yan, D., S. Chen, and Y. Liu. Heat resistance of MKG. *Metakaolin-based geopolymers: design, mechanisms and performance*, Springer Nature Singapore, Singapore, 2024, pp. 159–179.

[41] Arslan, F., A. Benli, and M. Karatas. Effect of high temperature on the performance of self-compacting mortars produced with calcined kaolin and metakaolin. *Construction and Building Materials*, Vol. 256, 2020, id. 119497.

[42] Jindal, B. B., D. Singhal, S. K. Sharma, and D. K. Ashish. Improving compressive strength of low calcium fly ash geopolymer concrete with alccofine. *Advances in Concrete Construction*, Vol. 5, No. 1, Techno-Press 2017, id. 17.

[43] Ashish, D. K. and S. K. Verma. Cementing efficiency of flash and rotary-calcined metakaolin in concrete. *Journal of Materials in Civil Engineering, American Society of Civil Engineers* 2019, id. 4019307.

[44] Dash, M. K., S. K. Patro, and A. K. Rath. Sustainable use of industrial-waste as partial replacement of fine aggregate for preparation of concrete – A review. *International Journal of Sustainable Built Environment*, Vol. 5, Elsevier B.V. 2016, pp. 484–516.

[45] Agrawal, D., U. P. Waghe, M. D. Goel, and A. Bagde. Effect of micro-silica and crumb rubber on mechanical properties of concrete. *Engineering Access*, Vol. 10, No. 2, 2024, pp. 189–196.

[46] Agrawal, D., U. P. Waghe, M. D. Goel, S. P. Raut, and R. Patil. Performance of geopolymer concrete developed using waste tire rubber and other industrial wastes: a critical review. *Recent Trends in Construction Technology and Management: Select Proceedings of ACTM 2021, 2022*, pp. 29–42.

[47] Agrawal, D., U. Waghe, K. Ansari, R. Dighade, M. Amran, D. N. Qader, et al. Experimental effect of pre-treatment of rubber fibers on mechanical properties of rubberized concrete. *Journal of Materials Research and Technology*, Vol. 23, 2023, pp. 791–807.

[48] Agrawal, D., U. Waghe, K. Ansari, M. Amran, Y. Gamil, A. E. Alluqmani, et al. Optimization of eco-friendly concrete with

recycled coarse aggregates and rubber particles as sustainable industrial byproducts for construction practices. *Helion*, Vol. 10, No. 4, 2024, pp. e25923–e25923.

[49] Ashish, D. K. and S. K. Verma. Robustness of self-compacting concrete containing waste foundry sand and metakaolin: A sustainable approach. *Journal of Hazardous Materials*, Vol. 401, 2021, id. 123329.

[50] Ashish, D. K., S. K. Verma, M. Ju, and H. Sharma. High volume waste foundry sand self-compacting concrete–Transitioning industrial symbiosis. *Process Safety and Environmental Protection*, Vol. 173, 2023, pp. 666–692Elsevier.

[51] Talati, I., K. J. Shah, O. Patel, J. Tanna, A. Jain, A. D. Oza, et al. Study of AQI monitoring system of indoor environment using machine learning model and IoT device, *Rocznik Ochrona Środowiska*, Vol. 27, 2025, pp. 152–163.

[52] Sharma, H., D. K. Ashish, and S. K. Sharma. Development of low-carbon recycled aggregate concrete using carbonation treatment and alccofine. *Energy, Ecology and Environment*, Vol. 9, No. 3, 2024, pp. 230–240.

[53] 269 IS. Ordinary Portland Cement Specification. IS 269-2015, New Delhi, India. 2015;Sixth Rev(December):1–14.

[54] 3IS 2386 P. Methods Of Test For Aggregates For Concrete Specific Gravity, Density, Voids, Absorption And Bulking. IS 2386 Part 3-2016, New Delhi, India. 1963;2386 Part(October 1963):1–19.

[55] 383 IS. Coarse and fine aggregate for concrete - Specification. Bureau of Indian Standards IS 383 -2016, New Delhi, India. 2016;(January):1–18.

[56] 5 IS 1199 P. Fresh Concrete-Methods of Sampling, Testing and Analysis Part 5 Making and Curing of Test Specimens (First Revision). IS 1199 Part 5-2018, New Delhi, India [Internet]. 2018;1199(December). Available from: [www.standardsbiso.in](http://www.standardsbiso.in)

[57] Elnemr, A. and R. Shaltout. Rheological and mechanical characterization of self-compacting concrete using recycled aggregate, *Materials*, Vol. 18, No. 7, 2024, id. 1519.

[58] 516 IS. Hardened concrete – Methods of test. IS 516-2021, New Delhi, India [Internet]. 2021;54(August):1–20. Available from: [www.standardsbiso.in](http://www.standardsbiso.in).

[59] 5816 IS. Specification for splitting tensile strength of concrete -Method of Test. IS 5816-1999, New Delhi, India. 1999, pp. 1–8.

[60] C1202. Standard Test Method for Electrical Indication of Concrete's Ability to Resist Chloride Ion Penetration 1. ASTM C1202. 2012; 10.1520/C1202-12.

[61] Patil, M. V. and Y. D. Patil. Effect of copper slag and granite dust as sand replacement on the properties of concrete. *Materials Today: Proceedings*, Vol. 43, 2021, pp. 1666–1677.

[62] Patil, M. V.. Properties and effects of copper slag in concrete. *International Journal of Advances in Mechanical and Civil Engineering*, Vol. 2, No. 2, 2015.

[63] Kurzekar, A. S., U. Waghe, K. Ansari, A. N. Dabhade, T. Biswas, S. Alguri, et al. Development and optimization of geopolymers-based artificial angular coarse aggregate using cut-blade mechanism. *Case Studies in Construction Materials*, Vol. 21, 2024, id. e03826.

[64] Waghe U., D. Agrawal, K. Ansari, M. Wagh, M. Amran, B. T. Alsulami, et al. Enhancing eco-concrete performance through synergistic integration of sugarcane, metakaolin, and crumb rubber: Experimental investigation and response surface optimization. *Journal of Engineering Research*, No. 12, No. 4, 2024, pp. 645–658.